Heliyon 9 (2023) e19352

Contents lists available at ScienceDirect

Heliyon

journal homepage: www.cell.com/heliyon

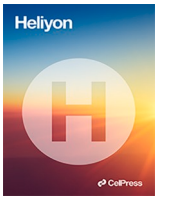

# A cuproptosis-related lncRNA signature for predicting prognosis and immune response in hepatocellular carcinoma

Jingyi Wu [a,1], Jianzuo Yao [b,1], Shu Jia [a], Xiaokun Yao [a], Jingping Shao [a], Weijuan Cao [a], Shuwei Ma [a], Xiaomin Yao [a,2,**], Hong Li [b,2,*]

[a] Faculty of Pharmacy, Zhejiang Pharmaceutical University, Ningbo, 315100, PR China
[b] Department of Hepatobiliary and Pancreatic Surgery, Li Huili Hospital Affiliated to Ningbo University, Ningbo, 315040, PR China

ARTICLE INFO

*Keywords:*
Bioinformatics
cuproptosis
lncRNA
Hepatocellular carcinoma
Immunotherapy

ABSTRACT

*Background:* Hepatocellular carcinoma (HCC) has a high incidence and poor prognosis. Cuproptosis is a novel type of cell death, which differs from previously reported types of cell death such as apoptosis, autophagy, proptosis, ferroptosis, necroptosis, etc. Long non-coding RNAs (lncRNAs) play multiple roles in HCC.

*Methods:* We downloaded information from The Cancer Genome Atlas (TCGA) database, and obtained cuproptosis-related genes from published studies. The cuproptosis-related lncRNAs were obtained by correlation analysis, and subsequently used to construct a prognostic cuproptosis-related lncRNA signature. Analyses of overall survival (OS), progression-free survival (PFS), receiver operating characteristic (ROC) curve with the area under the curve (AUC) values and the index of concordance (c-index) curve were used to evaluate the signature. The tumor microenvironment (TME) was analyzed by ESTIMATE algorithm. The immune cell data was downloaded from the Tumor Immune Estimation Resource (TIMER) 2.0 database. Immune-related pathways were analyzed by single-sample gene set enrichment analysis (ssGSEA) algorithm. Immunophenoscore (IPS) scores from The Cancer Immunome (TCIA) database were used to evaluate immunotherapy response. The "pRRophetic" was employed to screen drugs for high-risk patients. The candidate lncRNA expression levels were detected by Real Time Quantitative PCR.

*Results:* We constructed a cuproptosis-related lncRNA signature containing seven lncRNAs: AC125437.1, PCED1B-AS1, PICSAR, AP001372.2, AC027097.1, LINC00479, and SLC6A1-AS1. This signature had excellent accuracy, and was independent of the stratification of clinicopathological features. Further study showed that high-risk tumors under this signature had higher TMB, fewer TME components and higher tumor purity. The tumors with high risk were not enriched in immune cell infiltration or immune process pathways, and high-risk patients had a poor response to immunotherapy. Moreover, 29 drugs such as sorafenib, dasatinib and paclitaxel were screened for high-risk HCC patients to improve their prognosis. The expression levels of the candidate lncRNAs in HCC tissue were significantly increased (except PCED1B-AS1).

* Corresponding author.
** Corresponding author. Faculty of Pharmacy, Zhejiang Pharmaceutical University, No. 888 Yinxian Avenue East Section, Ningbo, 315000, China.
*E-mail addresses:* yaoxiaomin780307@163.com, yaoxm@zjpc.net.cn (X. Yao), lancet2017@163.com, lhllihong@nbu.edu.cn (H. Li).
[1] Jingyi Wu and Jianzuo Yao are Co-first authors, who contributed equally.
[2] Xiaomin Yao and Hong Li are Co-corresponding authors, who contributed equally.

https://doi.org/10.1016/j.heliyon.2023.e19352
Received 2 January 2023; Received in revised form 9 August 2023; Accepted 20 August 2023
Available online 29 August 2023

*Conclusions:* Our prognostic cuproptosis-related lncRNA signature was accurate and effective for predicting the prognosis of HCC. The immunotherapy was unsuitable for high-risk HCC patients with this signature.

## 1. Introduction

Primary liver cancer has the sixth highest incidence among tumors and the third highest mortality worldwide, of which the predominant subtype is hepatocellular carcinoma (HCC), which has a poor prognosis [1,2]. In recent years, major progress has been made in the treatment of HCC by various modalities such as surgery, chemotherapy, targeted therapy and immunotherapy, but the 5-year survival rate of HCC remains below 30% [3]. Therefore, it is critical to conduct prognosis-related studies for HCC.

The intracellular copper concentration is maintained at extremely low levels under physiological conditions, and intracellular copper accumulation leads to cell death by previously unknown mechanisms. Based on this idea, several agents that could increase intracellular copper concentration, termed copper ionophores (such as elesclomol, disulfuram, 7-iodo-5-chloro-8-hydroxyquinoline, etc.), have been used for anti-tumor therapy [4]. However, a phase 3 clinical trial of melanoma showed poor effects of elesclomol, which may be related to the unknown molecular mechanisms of elesclomol resulting in failure to select an appropriate patient population [5,6]. Tsvetkov et al. recently revealed that elesclomol-mediated intracellular copper accumulation leading to cancer cell death was achieved by copper directly binding to the lipoyl moiety of lipoylated proteins of the tricarboxylic acid (TCA) cycle, which they termed as cuproptosis [6]. In addition, the susceptibility of copper-mediated cell death was linked to ferrodoxin-1 (FDX1) and lipoylated protein levels in human cancer cells, and this correlation could contribute to patient selection for the application of copper ionophores [6,7]. As a new form of cell death, cuproptosis may provide new strategies for tumor treatment. Hence, it is critical to understand the underlying mechanism of cuproptosis.

Long non-coding RNAs (lncRNAs) are a group of RNA transcripts comprising more than 200 nucleotides that do not encode proteins [8]. They have attracted considerable attention in recent years due to their involvement in numerous regulatory pathways of cellular functions and disease progression. In addition, lncRNAs play vital roles in HCC including regulation of tumorigenesis and progression by multiple mechanisms such as promotion or prevention of stemness, proliferation, metastasis and drug resistance of HCC, indicating their substantial potential for diagnostic and therapeutic applications in HCC [9,10]. With the assistance of bioinformatics, the utilization of lncRNAs to construct models to predict prognosis and other phenotypes of cancer patients has achieved satisfactory results. For HCC, recent studies have described several lncRNA prognostic models related to different processes, such as ferroptosis, N-6 methylation, early recurrence, etc [11–13]. The study of lncRNAs related to cuproptosis contributes to a deeper understanding of cuproptosis and its function.

## 2. Materials and methods

### 2.1. Datasets acquisition and processing

In this study, we aimed to construct a cuproptosis-related lncRNA signature to predict the prognosis of HCC patients, analyze the tumor mutation burden (TMB) and immune features of high-risk patients, and finally screen highly sensitive drugs to improve the prognosis.

The information including RNA-seq transcriptome data, clinical data and simple nucleotide variation data of liver hepatocellular carcinoma (LIHC) patients was obtained from The Cancer Genome Atlas (TCGA) database, which includes 374 tumor samples and 50 normal tissue samples. The Perl language was used to convert the form of data expression (Ensembl ID transformation to Gene Symbol) of the samples and distinguish between mRNA and lncRNA in every sample. The cuproptosis-related genes were identified from three studies [6,14,15]. All the revisions have been appropriately made. The result files of various immune cell infiltration calculated with different algorithms were downloaded from the Tumor Immune Estimation Resource 2.0 database (TIMER2.0, http://timer.comp-genomics.org/). The file with Immunophenoscore (IPS) scores of every sample was acquired from The Cancer Immunome database (TCIA, https://tcia.at). All the unknown or unspecified data were removed.

### 2.2. Bioinformatics and statistical analysis

#### 2.2.1. Construction of a prognostic cuproptosis-related lncRNAs signature and a nomogram

The data analysis and result visualization were accomplished in R version 4.1.0. The "limma" R package was used to analyze the correlation of every lncRNA and cuproptosis-related genes by the Wilcoxon test and identify the cuproptosis-related lncRNAs under the screening criteria as correlation coefficient $|R| > 0.4$ and $p < 0.001$.

All the tumor samples were randomly and equally divided into two cohorts called the training set and the test set, respectively. In the training set, the correlation between every cuproptosis-related lncRNA expression level and prognosis of HCC patients was calculated by univariate Cox regression. Thereafter, seven lncRNAs with prognostic significance ($p < 0.05$) and the corresponding risk coefficients were employed for construction of cuproptosis-related lncRNAs by least absolute shrinkage and selection operator (LASSO) analysis. The formula was established as follows: Risk score = lncRNA1 risk coefficient × lncRNA1 expression + lncRNA2 risk coefficient × lncRNA2 expression + … + lncRNAn risk coefficient × lncRNAn expression. Risk score of every tumor sample was

computed based on the formula. Thereafter, all tumor samples were divided into the high-risk and low-risk groups according to the median risk score.

A nomogram was constructed by the "rms" R package to predict the 1-year, 3-year, and 5-year OS rates of HCC patients, and the corresponding calibration curve was used to evaluate the accuracy of the nomogram.

### 2.2.2. *Evaluation of the prognostic cuproptosis-related lncRNAs signature*

Differences in seven clinical traits between the training set and test set were analyzed by chi-squared test to provide a precondition

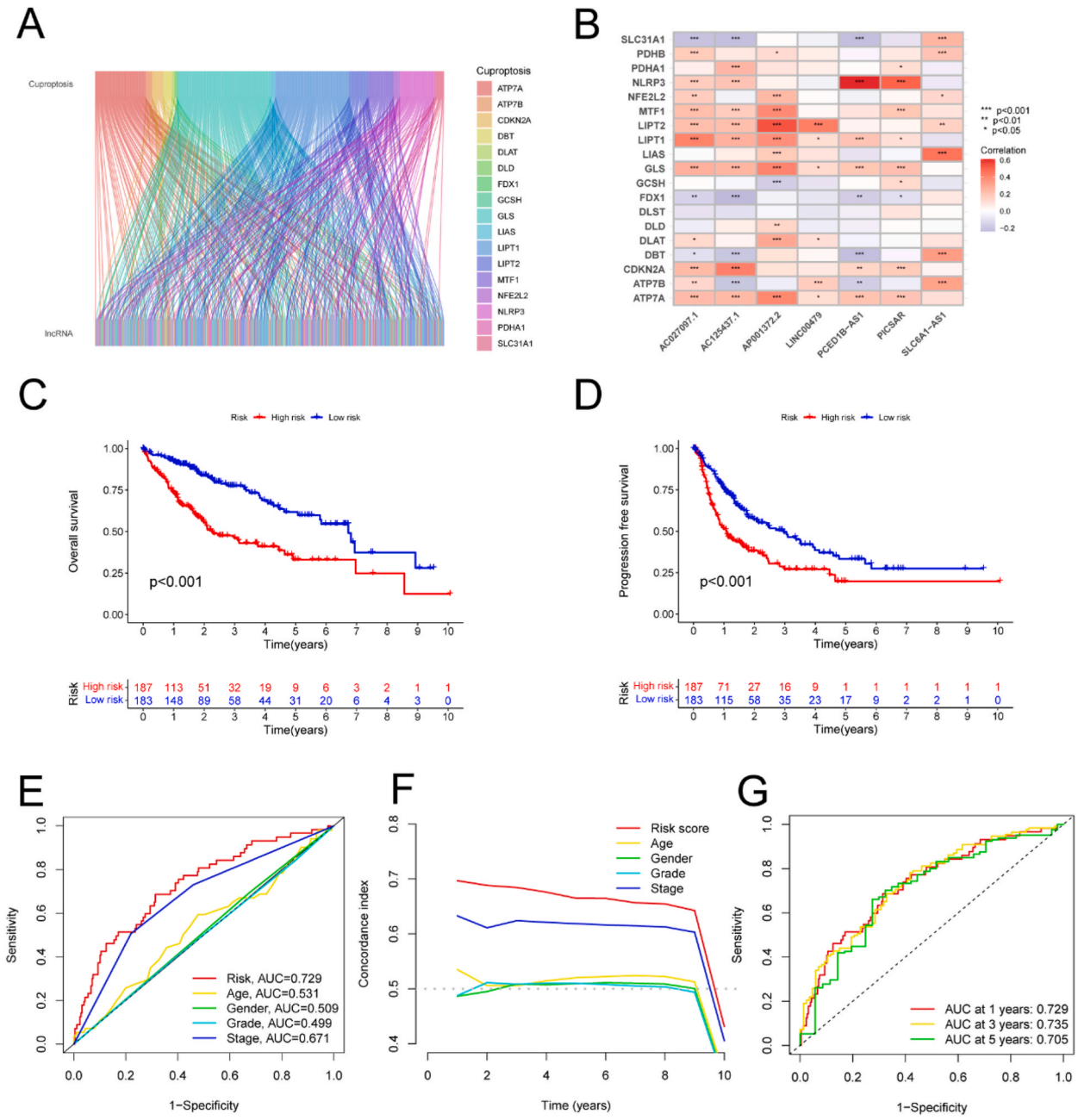


**Fig. 1.** Construction of a prognostic cuproptosis-related lncRNAs signature and evaluation of the accuracy of the signature. (A) The Sankey diagram of the connection degree between the cuproptosis-related lncRNAs and cuproptosis-related genes. (B) The heat map of the correlation between 7 prognostic signature lncRNAs and cuproptosis-related genes. (C) Overall survival curve between the high-risk and low-risk groups in all samples. (D) Progression free survival curve between the high- and low-risk group in all samples. (E) ROC curve and AUCs of comparison the prognostic accuracy of the signature and clinical features in all samples. (F) *C*-index curve of comparison the prognostic accuracy of the signature and clinical features in all samples. (G) ROC curve and AUCs at 1-year, 3-years and 5-years survival in all samples. *, $P < 0.05$; **, $P < 0.01$; ***, $P < 0.001$.

for internal validation. The survival analyses were conducted by "survival" and "survminer" R packages for tumor samples to verify the prognostic validity of this signature. The receiver operating characteristic (ROC) curves with the area under the curve (AUC) values and index of concordance (c-index) were drawn to evaluate the accuracy performance of the signature.

#### 2.2.3. Exploring patient features under the prognostic cuproptosis-related lncRNAs signature

Tumor mutation burden (TMB) of every tumor sample was computed by the Perl language and then visualized with the "maftools" R package (only the top 10 TM B genes are shown). The "estimate" R package was performed to compute the tumor microenvironment (TME) score of every tumor sample. The analysis of immune cell infiltration in tumor was completed by the Wilcoxon test (only shown with $p < 0.05$). The single-sample gene set enrichment analysis (ssGSEA) was employed to calculate the scores of immune-related pathways with the "gsva" R package. Finally, the "pRRophetic" R package was employed to screen for appropriate drugs to guide clinical treatment (Wilcoxon test, filtered at $p < 0.001$).

### 2.3. Real time quantitative polymerase chain reaction (RT-qPCR) assay

Total RNA was extracted from 12 pairs HCC specimens using RNA-easy Isolation Reagent (Vazyme Biotech Co., Ltd). The cDNA was produced using a total of 1 μg of RNA with the HiScript III All-in-one RT SuperMix kit (Vazyme Biotech Co., Ltd). Finally, the gene expression was examined using the ChamQ SYBR Mixture real-time detection system. The reaction mixture in a volume of 20 μl as follows: cDNA (1 μl), ChamQ SYBR Color qPCR Master Mix (10 μl, Vazyme Biotech), and 0.4 μl of each primer (10 μM). The amplification conditions were as follows: 95 °C (30 s), followed by 40 cycles of 95 °C (15 s) and 60 °C (30 s), then 95 °C (15 s), 60 °C (60 s) and 95 °C (15 s). The primers are listed in Table 3. All data were expressed as mean ± standard error (SE) and analyzed by SPSS22.0 using T test. Then the chart drew by Graph Pad Prism 9.0 software. Statistical significance was set at $p < 0.05$.

## 3. Results

### 3.1. Construction of a prognostic cuproptosis-related lncRNAs signature and evaluation of the accuracy of the signature

Based on the cuproptosis-related genes identified from published studies, we identified 497 cuproptosis-related lncRNAs for further study (Fig. 1A and Supplementary Table 1). Thereafter, 74 cuproptosis-related lncRNAs related to the prognosis of HCC samples were obtained in the training set (Supplementary Table 2). Subsequently, the prognostic cuproptosis-related lncRNA signature was identified, and the risk score of every tumor sample was calculated with the following formula: 1.11872513217005 × AC125437.1 expression - 1.03411888545497 × PCED1B-AS1 expression +0.491369364434185 × PICSAR expression +0.563760741613278 × AP001372.2 expression +1.00627516701855 × AC027097.1 expression +1.25937962745877 × LINC00479 expression - 0.937864168024504 × SLC6A1-AS1 expression. Correlation between the seven prognostic signature lncRNAs and cuproptosis-related genes is shown in Fig. 1B. OS and PFS were analyzed in all tumor samples, which showed that the OS and PFS of high-risk group patients were significantly shorter ($p < 0.001$, Fig. 1C and D). The ROC and *C*-index curves were used to evaluate the prediction

**Table 1**
The clinicopathological characteristics of patients in different cohorts.

| Covariates | Type | Total | Test | Train | Pvalue |
|---|---|---|---|---|---|
| Age | ≤65 | 232 (62.7%) | 117 (63.24%) | 115 (62.16%) | 0.9144 |
| | >65 | 138 (37.3%) | 68 (36.76%) | 70 (37.84%) | |
| Gender | FEMALE | 121 (32.7%) | 61 (32.97%) | 60 (32.43%) | 1 |
| | MALE | 249 (67.3%) | 124 (67.03%) | 125 (67.57%) | |
| Grade | G1 | 55 (14.86%) | 24 (12.97%) | 31 (16.76%) | 0.642 |
| | G2 | 177 (47.84%) | 90 (48.65%) | 87 (47.03%) | |
| | G3 | 121 (32.7%) | 64 (34.59%) | 57 (30.81%) | |
| | G4 | 12 (3.24%) | 5 (2.7%) | 7 (3.78%) | |
| | unknow | 5 (1.35%) | 2 (1.08%) | 3 (1.62%) | |
| Stage | Stage I | 171 (46.22%) | 84 (45.41%) | 87 (47.03%) | 0.3627 |
| | Stage II | 85 (22.97%) | 38 (20.54%) | 47 (25.41%) | |
| | Stage III | 85 (22.97%) | 49 (26.49%) | 36 (19.46%) | |
| | Stage IV | 5 (1.35%) | 2 (1.08%) | 3 (1.62%) | |
| | unknow | 24 (6.49%) | 12 (6.49%) | 12 (6.49%) | |
| T | T1 | 181 (48.92%) | 90 (48.65%) | 91 (49.19%) | 0.2803 |
| | T2 | 93 (25.14%) | 41 (22.16%) | 52 (28.11%) | |
| | T3 | 80 (21.62%) | 47 (25.41%) | 33 (17.84%) | |
| | T4 | 13 (3.51%) | 6 (3.24%) | 7 (3.78%) | |
| | unknow | 3 (0.81%) | 1 (0.54%) | 2 (1.08%) | |
| M | M0 | 266 (71.89%) | 143 (77.3%) | 123 (66.49%) | 0.5225 |
| | M1 | 4 (1.08%) | 1 (0.54%) | 3 (1.62%) | |
| | unknow | 100 (27.03%) | 41 (22.16%) | 59 (31.89%) | |
| N | N0 | 252 (68.11%) | 136 (73.51%) | 116 (62.7%) | 1 |
| | N1 | 4 (1.08%) | 2 (1.08%) | 2 (1.08%) | |
| | unknow | 114 (30.81%) | 47 (25.41%) | 67 (36.22%) | |

accuracy of the signature in all tumor samples, which revealed that the signature was superior to other clinicopathological features (Fig. 1E and F). The AUC reached 0.729 at 1-year, 0.735 at 3-years, and 0.705 at 5-years (Fig. 1G).

### 3.2. Internal validation of the prognostic cuproptosis-related lncRNAs signature

There was no difference in clinicopathological characteristics of samples between the training set and the test set (Table 1). In the

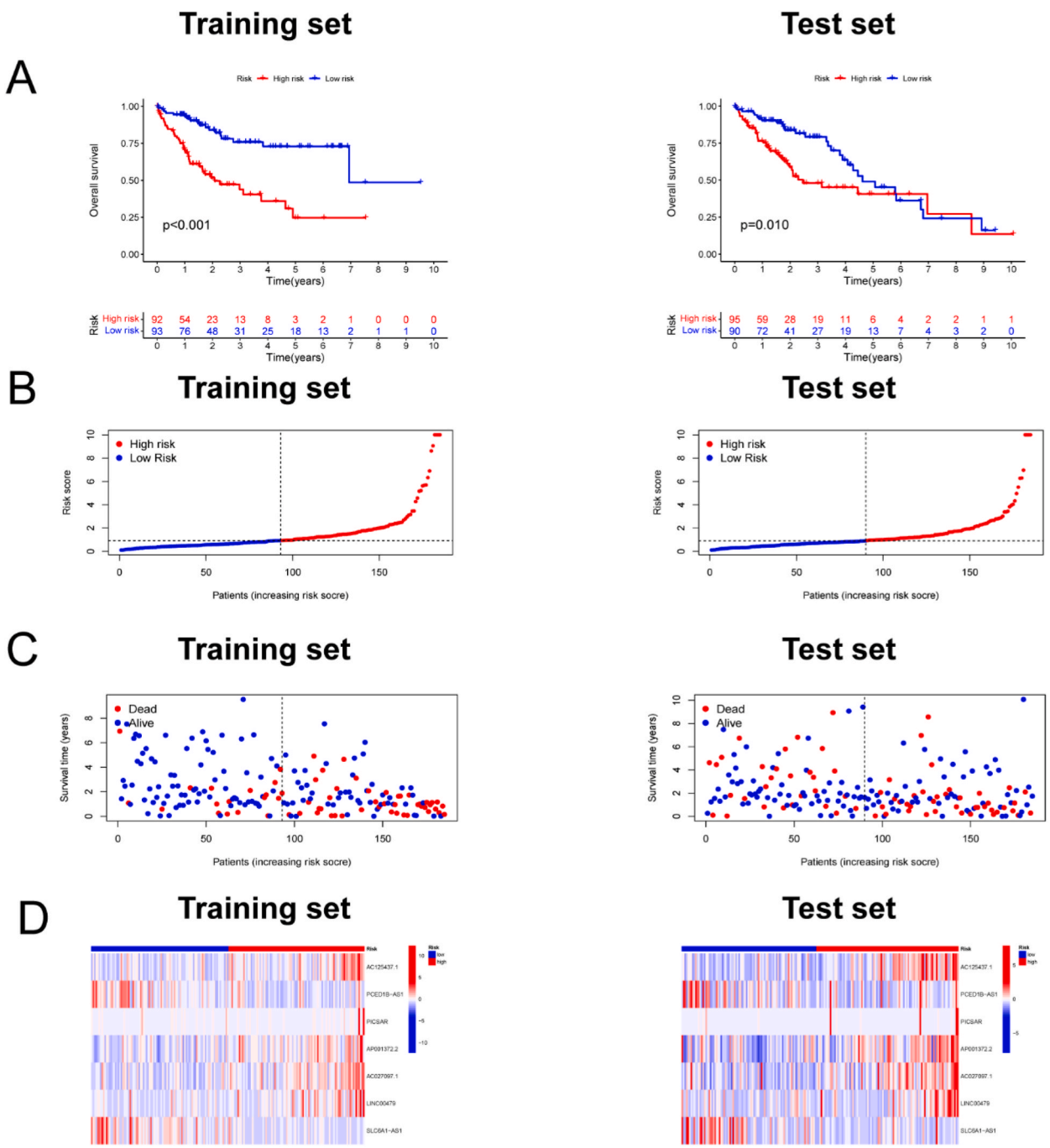


**Fig. 2.** Internal validation of the prognostic cuproptosis-related lncRNAs signature. (A) Overall survival curve between the high- and low-risk groups in the training set (left) and test set (right). (B) The distribution of risk scores for HCC samples in different sets. (C) The survival status of patients with differential risk scores in different sets. The blue points represent survivors, and the red points represent deaths. (D) The heat map of the 7 prognostic signature lncRNAs expression under differential risk groups in different sets.

training set, patients in the high-risk group had significantly shorter OS than patients in the low-risk group ($p < 0.001$), and the same outcome was obtained in the test set ($p = 0.01$, Fig. 2A). The risk scores of samples calculated by this signature were consistently distributed in the two different sets (Fig. 2B). Both the training and test sets showed that the number of deaths was higher in the high-risk group (Fig. 2C). The expression levels of seven lncRNAs identified in the signature showed the same trend in the two different sets (Fig. 2D).

### 3.3. Relationship between the prognostic cuproptosis-related lncRNAs signature and the clinicopathological features

Subgroup analyses of clinicopathological features including age, gender, grade and stage were performed. Survival analyses of each clinicopathological subgroup revealed that patients in the high-risk group had significantly shorter OS than patients in the low-risk group (Fig. 3A–D). Tumors in the high-risk group had a higher stage ($p < 0.01$) and grade ($p < 0.05$), and the higher stage was contributed by the T stage ($p < 0.001$), while the N stage and M stage had no effect (Fig. 3E).

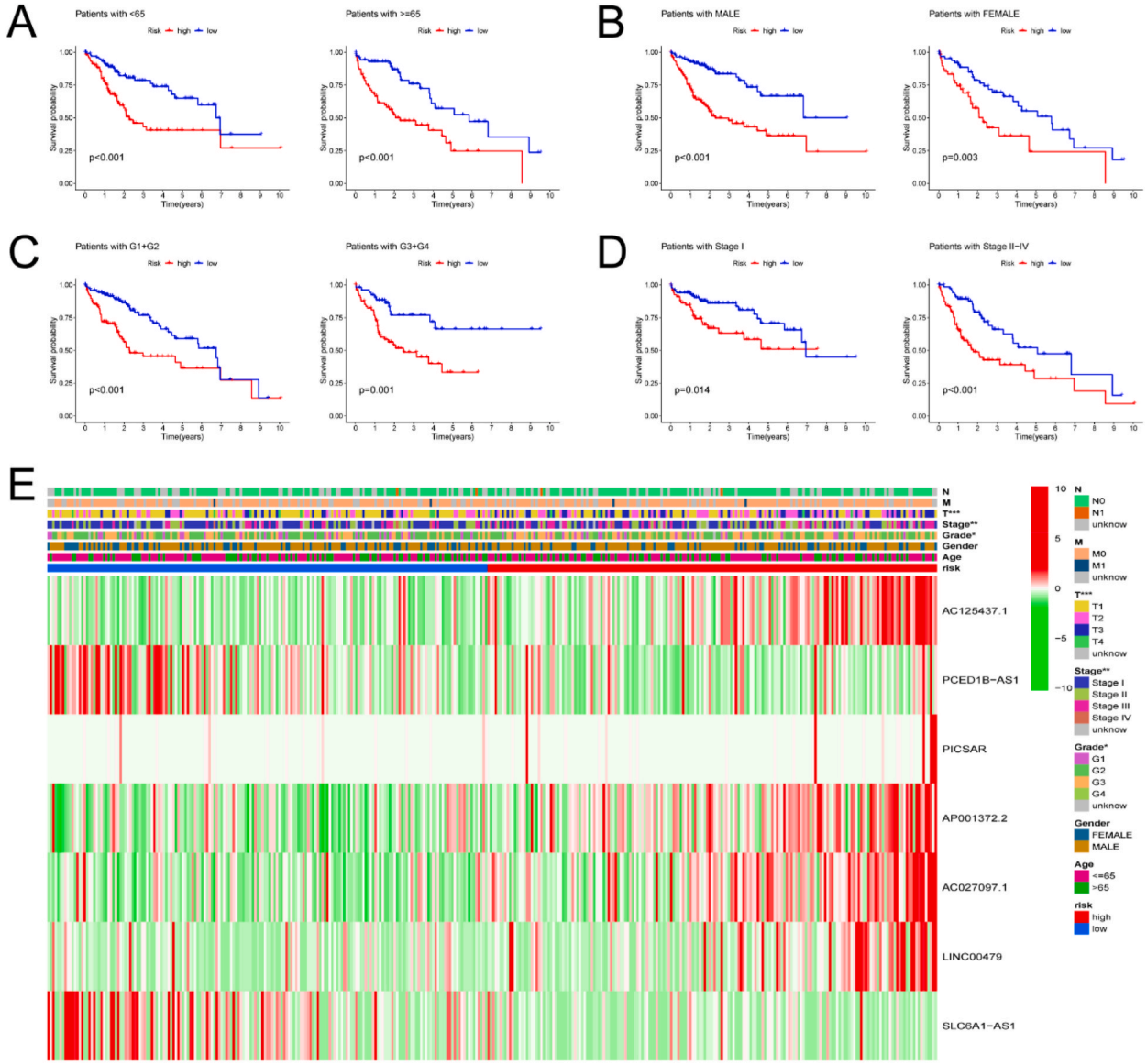


**Fig. 3.** Relationship between the prognostic cuproptosis-related lncRNAs signature and the clinicopathological features. (A–D) Survival analysis in differential risk groups of subgroups of each clinicopathological feature. (E) Distribution heat map of 7 prognostic signature lncRNAs and clinicopathological features in differential risk groups. *, $P < 0.05$; **, $P < 0.01$; ***, $P < 0.001$.

### 3.4. Construction and evaluation of a nomogram based on the prognostic cuproptosis-related lncRNAs signature

A nomogram predicting the prognosis of HCC patients at 1-year, 3-years, and 5-years was established, including differential risk groups and several clinicopathological features. The nomogram showed that the risk and stage levels had a significant effect on the prognosis of HCC patients ($p < 0.001$, Fig. 4A). The calibration curves were drawn to evaluate the consistency between the actual OS rate and predicted survival rate, and the result demonstrated good accuracy of this nomogram (Fig. 4B).

### 3.5. Tumor mutation burden in differential risk groups under the prognostic cuproptosis-related lncRNAs signature

The waterfall plots were used to assess whether a gene was mutated and the specific form of mutation in every tumor sample. *TP53*, *CTNNB1* and *TTN* were the top three mutated genes in the differential risk groups, and the number of mutations in these three genes was higher in the high-risk group (Fig. 5A–B). The TMB level was notably higher in the high-risk group ($p = 0.013$, Fig. 5C). Survival analysis based on the combination of TMB and risk scores showed that patients with high TMB level in the high-risk group had the worst prognosis ($p < 0.001$, Fig. 5D).

### 3.6. Tumor microenvironment in differential risk groups under the prognostic cuproptosis-related lncRNAs signature

To further investigate the tumor characteristics under the prognostic cuproptosis-related lncRNA signature, we performed TME analysis. The results revealed that the TME-related scores (including ESTIMATE score, Stromal score and Immune score) were higher in the low-risk group ($p < 0.001$, Fig. 6A–C), while the Tumor Purity score was higher in the high-risk group ($p < 0.001$, Fig. 6D).

### 3.7. Immunity analyses in differential risk groups under the prognostic cuproptosis-related lncRNAs signature

To further explore the correlation between the risk score and immune response, we analyzed the levels of immune cell infiltration, immune-related pathways and immune checkpoints in the high-risk and low-risk groups, and then predicted the effect of immunotherapy in differential risk groups. Among the various algorithms, most types of immune cell infiltration levels were shown to be higher in the low-risk group ($p < 0.05$, Fig. 7A). Meanwhile, the heat map of 13 conventional immune-related pathways showed tumors in the low-risk group had more active immune function ($p < 0.001$, Fig. 7B). There was a substantial difference in the expression level of immune checkpoints between the two differential risk groups and the low-risk group had higher expression of immune checkpoints, while only CD276 expression was higher in the high-risk group ($p < 0.05$, Fig. 7C). The effect of immunotherapy under the cuproptosis-related lncRNA signature indicated that patients in the low-risk group had higher immunotherapy scores for four types of

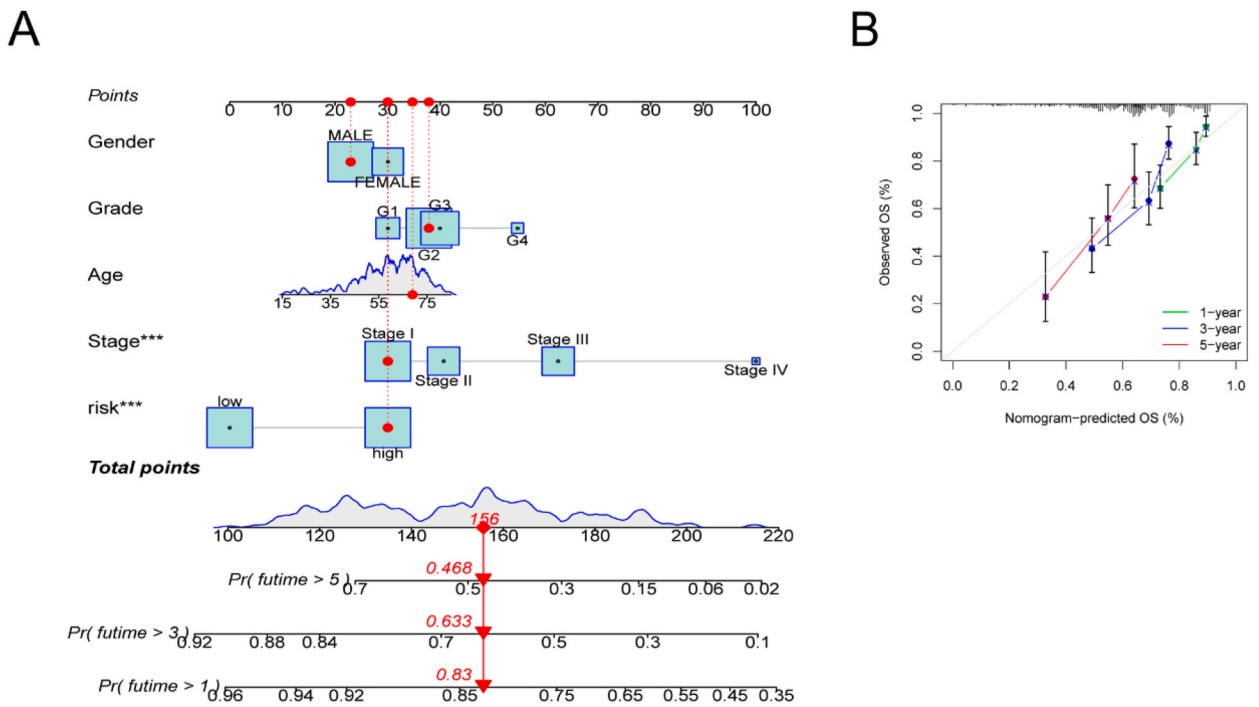


**Fig. 4.** Construction and evaluation of a nomogram based on the prognostic cuproptosis-related lncRNAs signature. (A) The nomogram combining differential risk groups and several clinicopathological features. (B) The calibration curve of evaluation the accuracy of the nomogram at 1, 3 and 5 years. ***, $P < 0.001$.

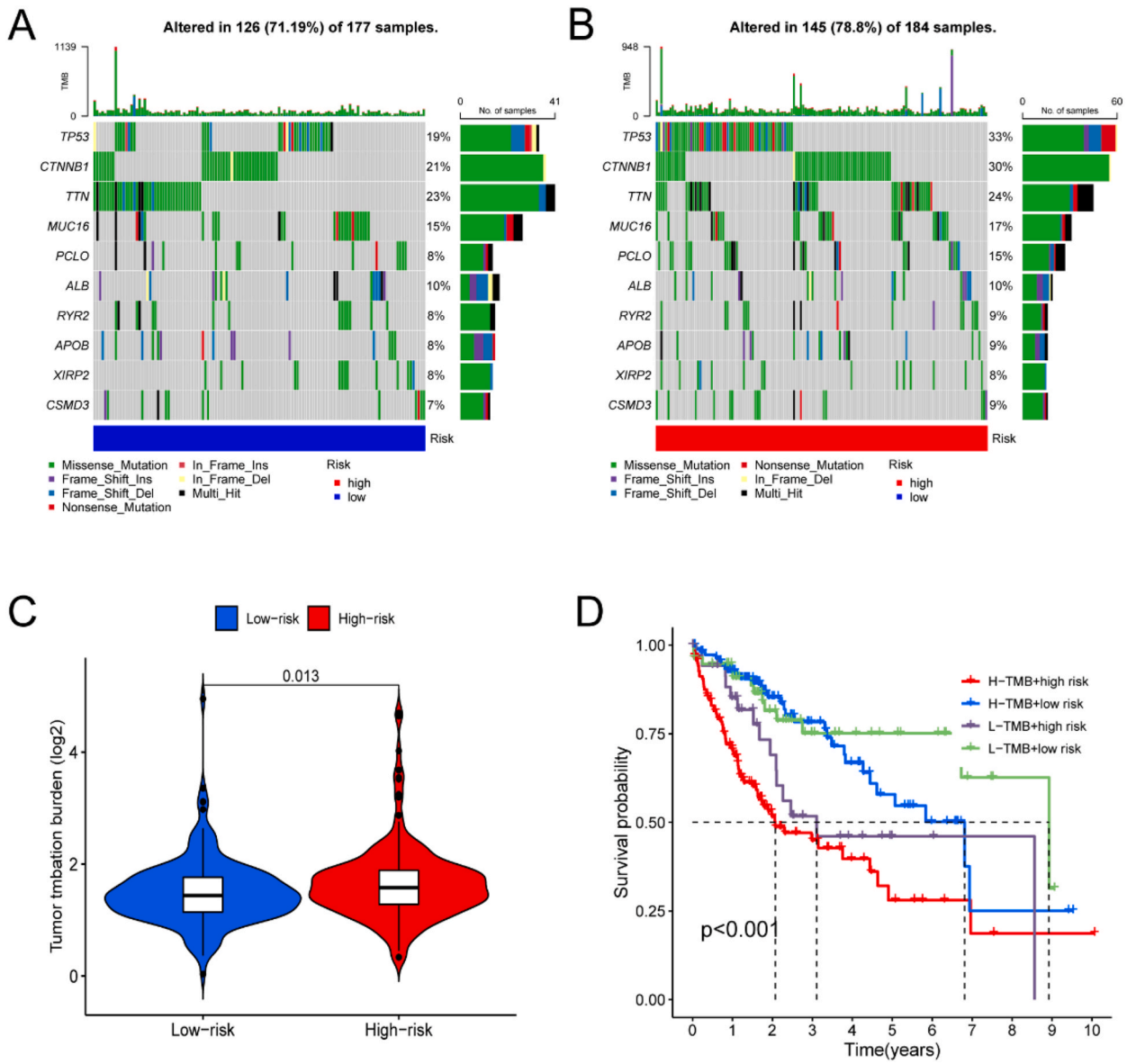


**Fig. 5.** Tumor mutation burden analysis in differential risk groups under the prognostic cuproptosis-related lncRNAs signature. (A–B) The waterfall plots showing mutation information of the top 10 TM B genes in each tumor sample of differential risk groups. (C) Difference of TMB level between high- and low-risk groups. (D) Overall survival curve based on the combination of TMB and risk scores.

immunotherapy, including no CTLA4 and PD1 treatment, PD1 treatment alone, CTLA4 treatment alone, combined PD1 and CTLA4 treatment ($p < 0.05$, Fig. 7D–G).

### *3.8. Screening appropriate drugs for high-risk patients identified in the prognostic cuproptosis-related lncRNAs signature*

To improve the prognosis of patients in the high-risk group, we screened 29 appropriate drugs for them ($p < 0.001$, Table 2). The results revealed that the top three drugs with the maximum correlation between risk scores of patients and drug sensitivity (IC50) were A−443,654, MG−132, and pyrimethamine, which act on Akt (protein kinase B), proteasome, and dihydrofolate reductase, respectively. Moreover, multiple kinase inhibitors including sorafenib, dasatinib and sunitinib were screened as potential drugs to improve the prognosis of high-risk patients.

### *3.9. Detecting the expression levels of the candidate lncRNAs in HCC tissue*

As illustrated in Fig. 8, the lncRNA expression levels of AC125437.1, PICSAR, AP001372.2, AC027097.1, LINC00479 and SLC6A1-

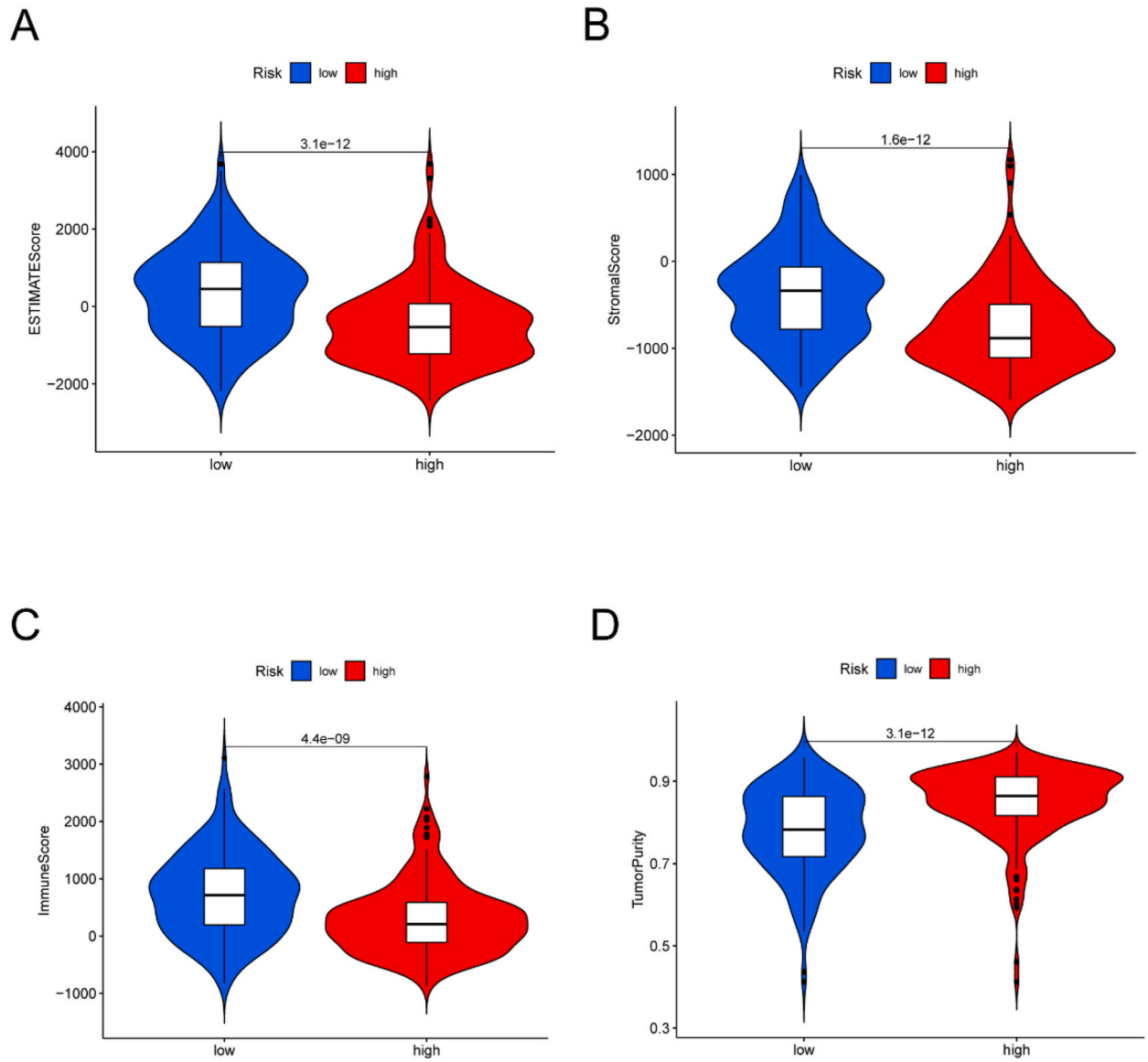


**Fig. 6.** Tumor microenvironment in differential risk groups under the prognostic cuproptosis-related lncRNAs signature. (A–D) TME-related scores (including ESTIMATE score, Stromal score and Immune score) and the Tumor purity score in the high- and low groups.

AS1 were obviously increased in the HCC tissue of 12 cases of HCC patients compared to the paracarcinoma tissue ($P < 0.05$; Fig. 8A, *C*-G). Moreover, the expression level of PCED1B-AS1 was decreased in HCC tissue compared to the paracarcinoma tissue but not significantly (Fig. 8B).

## 4. Discussion

HCC is characterized by high incidence and poor prognosis, which constitutes a major threat to human health. Cuproptosis, a new form of cell death, may offer new ideas for the treatment of malignant tumors. Herein, we first constructed a prognostic cuproptosis-related lncRNA signature and analyzed the characteristics of patients with poor prognosis. Based on the TCGA database, we randomly divided the data into two groups without clinical differences, namely the training set and the test set, and then identified cuproptosis-related lncRNAs. We employed seven lncRNAs (AC125437.1, PCED1B-AS1, PICSAR, AP001372.2, AC027097.1, LINC00479, SLC6A1-AS1) to construct a prognostic cuproptosis-related lncRNA signature in HCC by the training set. Studies have shown that PCED1B-AS1 induces immunosuppression of HCC by sponging hsa-miR-194–5p to enhance the expression of PD-L1 and PD-L2 [16]. PICSAR regulates tumorigenesis of HCC by sponging miR-588 to enhance the expression of eukaryotic initiation factor 6 (EIF6), resulting in activation of the PI3K/AKT/mTOR pathway [17]. Other prognostic cuproptosis-related lncRNAs in this signature have not been

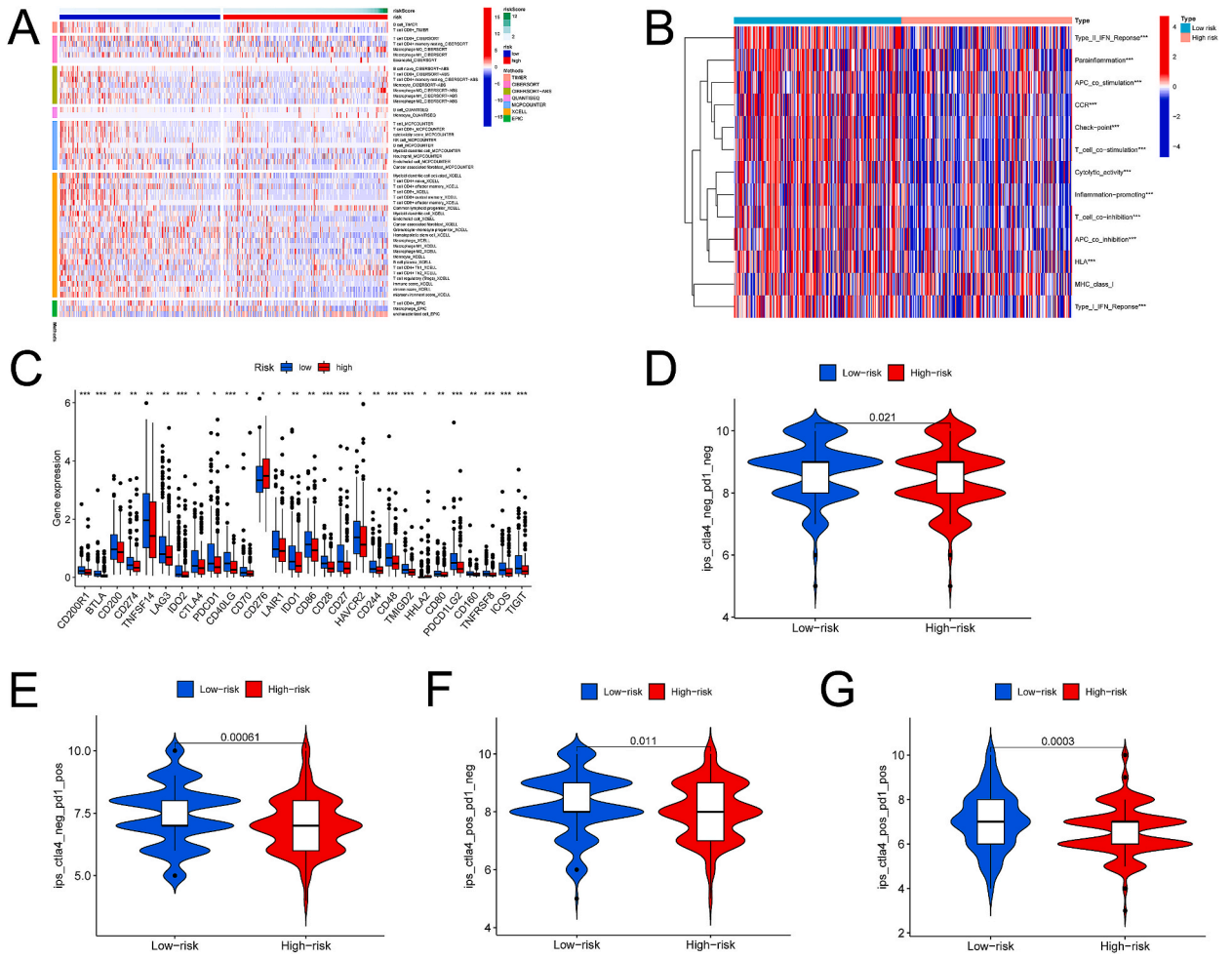


**Fig. 7.** Immune response in differential risk groups under the prognostic cuproptosis-related lncRNAs signature. (A) The heat map of immune cell infiltration in the high- and low-risk groups with various algorithms. (B) The heat map of immune-related pathways in the high- and low-risk groups. (C) Differences in the expression of immune checkpoints between the high- and low-risk groups. (D) Differences in the immunotherapy score without CTLA4 and PD1 treatment between the high- and low-risk groups. (E) Differences in the immunotherapy score with PD1 treatment alone between the high- and low-risk groups. (F) Differences in the immunotherapy score with CTLA4 treatment alone between the high- and low-risk groups. (G) Differences in the immunotherapy score with combined PD1 and CTLA4 treatment between the high- and low-risk groups. *, $P < 0.05$; **, $P < 0.01$; ***, $P < 0.001$.

reported, implying that their biological functions, particularly their specific role in cuproptosis, in HCC should be investigated.

Under this signature, every patient was assigned a risk score, and all patients were divided into two groups, the high-risk group and the low-risk group, by a median of the scores for further study. This signature can be used to accurately predict the prognosis of HCC patients, as evidenced by the shorter OS and PFS of patients in the high-risk group and the superior predictive effect of this signature compared to other clinicopathological features. Moreover, the predictive efficacy of this signature passed internal validation and was not affected by clinicopathological features including age, gender, stage and grade.

Analysis of TMB differences was used to study the characteristics of patients with poor prognosis. Previous studies have suggested that high TMB in various tumors can stimulate antigen formation and immune cell infiltration, subsequently enhancing immunotherapeutic efficacy and improving patient prognosis [18–20]. However, it has been shown that high TMB predicts neither immune checkpoint blockade response nor survival time in HCC patients [21,22]. In this study, the type of mutation genes (top 10) were consistent in the differential risk groups, and patients in the high-risk group who represented worse prognosis had a higher TMB. Further survival analysis in combination with TMB showed that high-risk group patients with high TMB had the worst prognosis, which could be applied to further study the prognosis of HCC patients and contribute to the development of an association between cuproptosis and TMB.

The tumor microenvironment (TME) means all components excluding cancer cells of solid tumors, and includes complex cellular and acellular components such as cancer-associated fibroblasts (CAFs), various immune cells, tumor vessels, extracellular matrix (ECM), etc [23]. These components contribute to the growth and progression of cancer cells and influence the prognosis of patients

**Table 2**
The appropriate drugs for high-risk patients identified in the prognostic cuproptosis-related lncRNAs signature.

| Description | Name | Cor[a] | P value |
|---|---|---|---|
| Multiple kinases inhibitor | Dasatinib | −0.26 | 4.3e−06 |
| | Sorafenib | −0.23 | 7.3e−06 |
| | Sunitinib | −0.21 | 5.7e−05 |
| Akt inhibitor | A−443,654 | −0.31 | 2e−09 |
| | AKT inhibitor VIII | −0.2 | 8.2e−05 |
| Lck/Src inhibitor | WH−4−023 | −0.25 | 1.4e−06 |
| | A−770,041 | −0.22 | 3.1e−05 |
| Microtubule-stabilizing agent | Paclitaxel | −0.26 | 4.4e−07 |
| | Epothilone B | −0.22 | 1.3e−05 |
| Proteasome inhibitor | MG−132 | −0.3 | 3.2e−09 |
| | Bortezomib | −0.26 | 3.9e−07 |
| Plk inhibitor | GW843682× | −0.27 | 2e−07 |
| Plk1 inhibitor | BI−2536 | −0.25 | 1.3e−06 |
| ERK inhibitor | FR−180,204 | −0.23 | 7.6e−06 |
| ERK5 inhibitor | BIX02189 | −0.22 | 2.2e−05 |
| Dihydrofolate reductase inhibitor | Pyrimethamine | −0.29 | 3.9e−08 |
| Inhibitor of the protein kinase cbeta isozyme | LY317615 | −0.26 | 6.4e−07 |
| Inhibitor of interleukin-2-inducible T cell kinase | BMS−509,744 | −0.26 | 3.3e−07 |
| Inhibitor of eIF-2α dephosphorylation | Salubrinal | −0.26 | 5.5e−07 |
| Ckit inhibitor | Masitinib | −0.24 | 3.3e−06 |
| Eg5 inhibitor | S−Trityl−L−cysteine | −0.23 | 5.8e−06 |
| MELK inhibitor | JW−7−52−1 | −0.23 | 6.2e−06 |
| Aurora kinase inhibitor | VX−680 | −0.22 | 1.6e−05 |
| MAP3K8 inhibitor | KIN001−266 | −0.22 | 2.4e−05 |
| CSF1 receptor inhibitor | GW−2580 | −0.22 | 2.6e−05 |
| CDK inhibitor | CGP−60,474 | −0.22 | 2.6e−05 |
| IGF-IR Inhibitor | GSK1904529 A | −0.21 | 4.2e−05 |
| JAK-3 inhibitor | KIN001−055 | −0.21 | 4.7e−05 |
| SERCA inhibitor | Thapsigargin | −0.2 | 9.7e−05 |

[a] Cor, Correlation between risk scores of patients and drug senstivity (IC50).

**Table 3**
Polymerase chain reaction primer sets in RT-qPCR.

| Gene | Primer sequences |
|---|---|
| AC125437.1 | Reverse TCTAAGGCAAGGTTGACAA |
| | Forward ACACAGAGACACAGAAGAC |
| PCED1B-AS1 | Reverse GGAAGCGGAAGACTAATGA |
| | Forward TACCACACCAGCAAGAAC |
| PICSAR | Reverse TGCCTCTTCCTCAGACAT |
| | Forward CTGGAGCCTCATTCACTG |
| AP001372.2 | Reverse GTACAACTACTATGGAGAACAG |
| | Forward ACTTAGGAGCGTGATTGC |
| AC027097.1 | Reverse ACGCTGATGATTAGTGACA |
| | Forward TTGTACTGGTGAGACTTGG |
| LINC00479 | Reverse CCACGAGGAAGTCAGGAT |
| | Forward TGCCACATTCAACATAACAC |
| SLC6A1-AS1 | Reverse TGAATAGTGCTGCTGTGAA |
| | Forward TTCTGCTTCTGAGTAGATACC |
| β-actin | Reverse GCTGATCCACATCTGCTGG |
| | Forward CATTGCTGACAGGATG |

with this disease [24,25]. In this study, the high-risk patients showed lower TME score and higher tumor purity score. This finding suggests that high-risk tumors contain more cancer cells and fewer TME components. In addition, the immune cells in TME are the fundamental basis for immunotherapy [24]. Immune-related analyses showed that high-risk tumors had lower number of immune cells, fewer immune process pathways, and lower expression of immune checkpoints except CD276, which implied that high-risk patients had lower immunogenicity in TME and worse response to immunotherapy. Targeted CD276 therapy might be beneficial for high-risk patients of HCC under this signature. Further studies with IPS scores confirmed that high-risk patients showed poorer response to immunotherapy (including no CTLA4 and PD1 treatment, PD1 treatment alone, CTLA4 treatment alone, and combined PD1 and CTLA4 treatment), suggesting that high-risk patients under this signature were unsuitable for immunotherapy.

Due to the poor response to immunotherapy in high-risk patients under this signature, we screened 29 appropriate drugs, including anti-tumor agents and targeted agents, to improve their prognosis. Among them, sorafenib was the first molecular targeted agent approved for patients with advanced HCC and the only available systemic therapy between 2007 and 2016 [26,27]. However, the OS of HCC remains poor after sorafenib administration. Overcoming sorafenib resistance is key to improving its efficacy in HCC. Previous

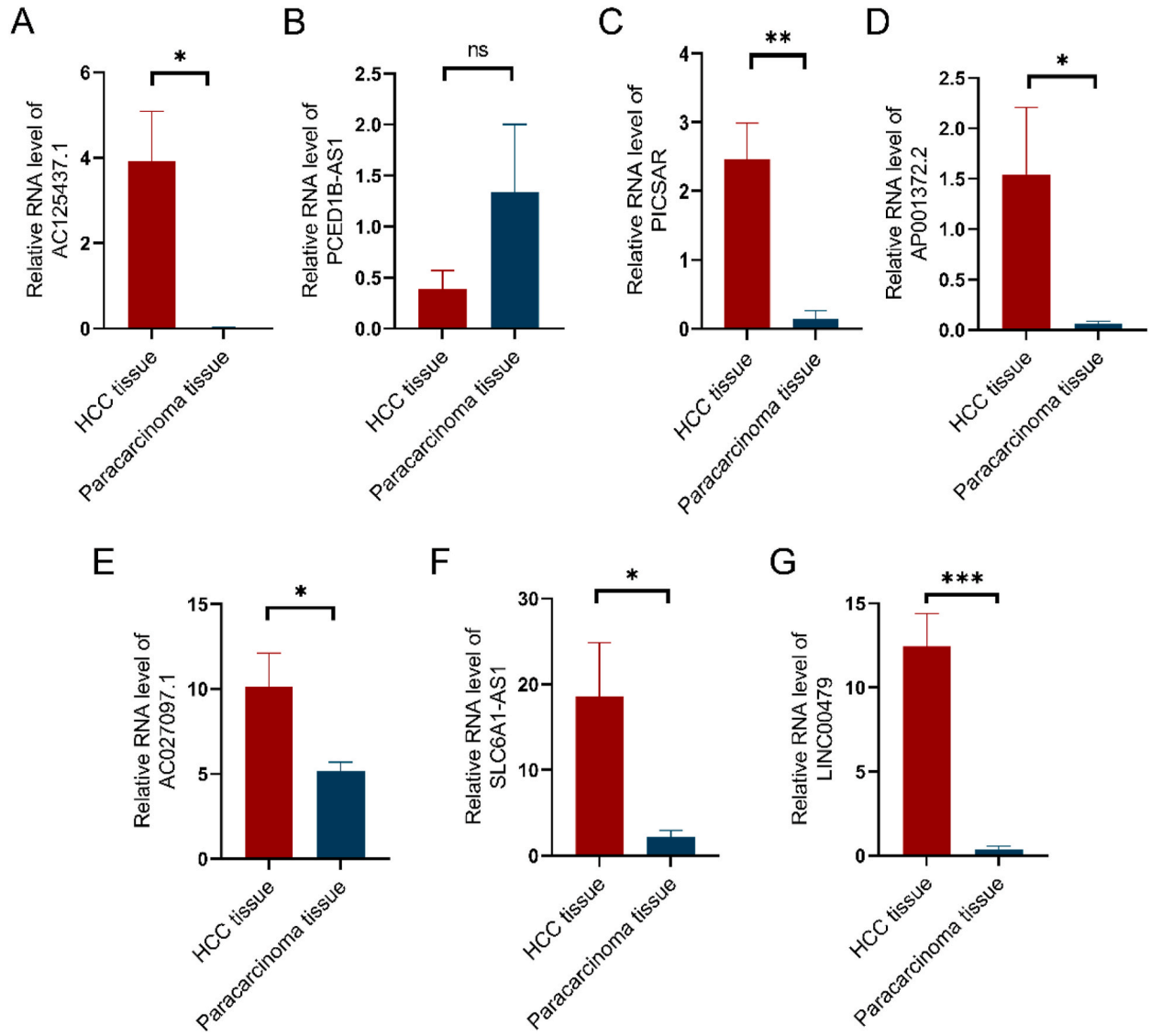


**Fig. 8.** The expression levels of the candidate lncRNAs in 12 pairs HCC specimens and paracarcinoma tissue. (A–G) Differences in the lncRNA expressions of AC125437.1, PCED1B-AS1, PICSAR, AP001372.2, AC027097.1, LINC00479, SLC6A1-AS1 in HCC and paracarcinoma tissue. *, $P < 0.05$; **, $P < 0.01$; ***, $P < 0.001$.

studies have reported that regulated cell death, particularly autophagy and ferroptosis, is involved in sorafenib resistance in HCC [28–31]. Cuproptosis, a new form of cell death, may provide an option for overcoming sorafenib resistance in advanced HCC patients and subsequently improve their OS. This study provides a new treatment option for high-risk patients under the prognostic cuproptosis-related lncRNA signature, which can potentially individualize treatment options for advanced HCC patients.

## 5. Conclusion

The cuproptosis-related lncRNA signature based on the TCGA database can predict the prognosis of HCC patients with excellent accuracy. Furthermore, tumors in the high-risk group under this signature showed higher TMB, fewer TME components, lower immune cell infiltration, fewer immune process pathways, and had a poor response to immunotherapy. Moreover, 29 drugs were screened for high-risk HCC patients to improve their prognosis. Finally, the expression levels of the candidate lncRNAs in HCC tissue were significantly increased (except PCED1B-AS1). This study provides important bioinformatics data for further experimental studies and clinical applications.

## Funding

This work was supported by Ningbo Digestive System Tumor Clinical Medicine Research Center (2019A21003), Project of Zhejiang Medical and Health Platform Plan (2022KY1079), Ningbo Science and Technology Program Public Welfare Project (2021S098, 2021S144), Ningbo Public Welfare Science & Technology Major Project (2021S106), Ningbo Natural Science Foundation Project (202003N4336, 202003N4337), Zhejiang Provincial Public Technology Research Projects (LGF22H310003) and Scientific Research Fund of Zhejiang Provincial Education Department (Y202250157).

## Consent for publication

The authors have no conflicts of interest to declare.

## Declarations

*Authors' contributions*

Conceived and designed the experiments: Jingyi Wu, Jianzuo Yao, Hong Li and Xiaomin Yao.
Performed the experiments: Jingyi Wu, Jianzuo Yao, Shu Jia, Xiaokun Yao, Jingping Shao, Weijuan Cao and Shuwei Ma.
Analyzed and interpreted the data: Jianzuo Yao, Jingyi Wu, Shu Jia, Weijuan Cao and Shuwei Ma.
Contributed reagents, materials, analysis tools or data: Jingyi Wu, Jianzuo Yao, Hong Li and Xiaomin Yao.
Wrote the paper: Jingyi Wu, Jianzuo Yao, Shu Jia, Jingping Shao, Xiaokun Yao, Weijuan Cao, Shuwei Ma, Hong Li and Xiaomin Yao. All authors have read and approved the manuscript.

*Data avaliability statement*

All data collected and analyzed in this study could be downloaded from public databases including TCGA (https://portal.gdc.cancer.gov/), TIMER2.0 (http://timer.comp-genomics.org/) and TCIA (https://tcia.at).

## Declaration of competing interest

The authors declare that they have no known competing financial interests or personal relationships that could have appeared to influence the work reported in this paper.

## Acknowledgement

We acknowledge Research Square Platform for making this manuscript as a preprint [32].

## Appendix A. Supplementary data

Supplementary data to this article can be found online at https://doi.org/10.1016/j.heliyon.2023.e19352.

## References

[1] H. Sung, J. Ferlay, R.L. Siegel, M. Laversanne, I. Soerjomataram, A. Jemal, F. Bray, Global cancer statistics 2020: GLOBOCAN estimates of incidence and mortality worldwide for 36 cancers in 185 Countries, CA A Cancer J. Clin. 71 (2021) 209–249, https://doi.org/10.3322/caac.21660.
[2] A.M. Moon, A.G. Singal, E.B. Tapper, Contemporary Epidemiology of Chronic liver disease and Cirrhosis, Clin. Gastroenterol. Hepatol. 18 (2020) 2650–2666, https://doi.org/10.1016/j.cgh.2019.07.060.
[3] J. Wang, J. Li, G. Tang, Y. Tian, S. Su, Y. Li, Clinical outcomes and influencing factors of PD-1/PD-L1 in hepatocellular carcinoma, Oncol. Lett. 21 (2021) 279, https://doi.org/10.3892/ol.2021.12540.
[4] V. Oliveri, Selective targeting of cancer cells by copper ionophores: an Overview, Front. Mol. Biosci. 9 (2022), 841814, https://doi.org/10.3389/fmolb.2022.841814.
[5] S.J. O'Day, A.M. Eggermont, V. Chiarion-Sileni, R. Kefford, J.J. Grob, L. Mortier, C. Robert, J. Schachter, A. Testori, J. Mackiewicz, P. Friedlander, C. Garbe, S. Ugurel, F. Collichio, W. Guo, J. Lufkin, S. Bahcall, V. Vukovic, A. Hauschild, Final results of phase III SYMMETRY study: randomized, double-blind trial of elesclomol plus paclitaxel versus paclitaxel alone as treatment for chemotherapy-naive patients with advanced melanoma, J. Clin. Oncol. 31 (2013) 1211–1218, https://doi.org/10.1200/jco.2012.44.5585.
[6] P. Tsvetkov, S. Coy, B. Petrova, M. Dreishpoon, A. Verma, M. Abdusamad, J. Rossen, L. Joesch-Cohen, R. Humeidi, R.D. Spangler, J.K. Eaton, E. Frenkel, M. Kocak, S.M. Corsello, S. Lutsenko, N. Kanarek, S. Santagata, T.R. Golub, Copper induces cell death by targeting lipoylated TCA cycle proteins, Science 375 (2022) 1254–1261, https://doi.org/10.1126/science.abf0529.
[7] P.A. Cobine, D.C. Brady, Cuproptosis: cellular and molecular mechanisms underlying copper-induced cell death, Mol. Cell 82 (2022) 1786–1787, https://doi.org/10.1016/j.molcel.2022.05.001.
[8] M.C. Bridges, A.C. Daulagala, A. Kourtidis, LNCcation: lncRNA localization and function, J. Cell Biol. 220 (2021), https://doi.org/10.1083/jcb.202009045.
[9] Z. Huang, J.K. Zhou, Y. Peng, W. He, C. Huang, The role of long noncoding RNAs in hepatocellular carcinoma, Mol. Cancer 19 (2020) 77, https://doi.org/10.1186/s12943-020-01188-4.

[10] J. He, S. Zhu, X. Liang, Q. Zhang, X. Luo, C. Liu, L. Song, LncRNA as a multifunctional regulator in cancer multi-drug resistance, Mol. Biol. Rep. 48 (2021) 1–15, https://doi.org/10.1007/s11033-021-06603-7.
[11] Z. Xu, B. Peng, Q. Liang, X. Chen, Y. Cai, S. Zeng, K. Gao, X. Wang, Q. Yi, Z. Gong, Y. Yan, Construction of a ferroptosis-related Nine-lncRNA signature for predicting prognosis and immune response in hepatocellular carcinoma, Front. Immunol. 12 (2021), 719175, https://doi.org/10.3389/fimmu.2021.719175.
[12] Y. Fu, X. Wei, Q. Han, J. Le, Y. Ma, X. Lin, Y. Xu, N. Liu, X. Wang, X. Kong, J. Gu, Y. Tong, H. Wu, Identification and characterization of a 25-lncRNA prognostic signature for early recurrence in hepatocellular carcinoma, BMC Cancer 21 (2021) 1165, https://doi.org/10.1186/s12885-021-08827-z.
[13] W. Zhao, Y. Yan, Z. Xiao, M. Wang, M. Xu, Z. Wang, Y. Wang, Z. Zhuang, D. Yang, G. Chen, G. Liang, Bicyclol ameliorates nonalcoholic fatty liver disease in mice via inhibiting MAPKs and NF-κB signaling pathways, Biomed. Pharmacother. 141 (2021), 111874, https://doi.org/10.1016/j.biopha.2021.111874.
[14] M.H. Emami, N. Sereshki, Z. Malakoutikhah, S.A.E. Dehkordi, A. Fahim, S. Mohammadzadeh, F. Maghool, Nrf 2 signaling pathway in trace metal carcinogenesis: a cross-talk between oxidative stress and angiogenesis, Comp. Biochem. Physiol. C Toxicol. Pharmacol. 254 (2022), 109266, https://doi.org/10.1016/j.cbpc.2022.109266.
[15] H. Deng, S. Zhu, H. Yang, H. Cui, H. Guo, J. Deng, Z. Ren, Y. Geng, P. Ouyang, Z. Xu, Y. Deng, Y. Zhu, The Dysregulation of Inflammatory pathways Triggered by copper Exposure, Biol. Trace Elem. Res. (2022), https://doi.org/10.1007/s12011-022-03171-0.
[16] F. Fan, K. Chen, X. Lu, A. Li, C. Liu, B. Wu, Dual targeting of PD-L1 and PD-L2 by PCED1B-AS1 via sponging hsa-miR-194-5p induces immunosuppression in hepatocellular carcinoma, Hepatol Int 15 (2021) 444–458, https://doi.org/10.1007/s12072-020-10101-6.
[17] Z. Liu, H. Mo, L. Sun, L. Wang, T. Chen, B. Yao, R. Liu, Y. Niu, K. Tu, Q. Xu, N. Yang, Long noncoding RNA PICSAR/miR-588/EIF6 axis regulates tumorigenesis of hepatocellular carcinoma by activating PI3K/AKT/mTOR signaling pathway, Cancer Sci. 111 (2020) 4118–4128, https://doi.org/10.1111/cas.14631.
[18] D. Miao, C.A. Margolis, N.I. Vokes, D. Liu, A. Taylor-Weiner, S.M. Wankowicz, D. Adeegbe, D. Keliher, B. Schilling, A. Tracy, M. Manos, N.G. Chau, G.J. Hanna, P. Polak, S.J. Rodig, S. Signoretti, L.M. Sholl, J.A. Engelman, G. Getz, P.A. Jänne, R.I. Haddad, T.K. Choueiri, D.A. Barbie, R. Haq, M.M. Awad, D. Schadendorf, F.S. Hodi, J. Bellmunt, K.K. Wong, P. Hammerman, E.M. Van Allen, Genomic correlates of response to immune checkpoint blockade in microsatellite-stable solid tumors, Nat. Genet. 50 (2018) 1271–1281, https://doi.org/10.1038/s41588-018-0200-2.
[19] R.M. Samstein, C.H. Lee, A.N. Shoushtari, M.D. Hellmann, R. Shen, Y.Y. Janjigian, D.A. Barron, A. Zehir, E.J. Jordan, A. Omuro, T.J. Kaley, S.M. Kendall, R. J. Motzer, A.A. Hakimi, M.H. Voss, P. Russo, J. Rosenberg, G. Iyer, B.H. Bochner, D.F. Bajorin, H.A. Al-Ahmadie, J.E. Chaft, C.M. Rudin, G.J. Riely, S. Baxi, A. L. Ho, R.J. Wong, D.G. Pfister, J.D. Wolchok, C.A. Barker, P.H. Gutin, C.W. Brennan, V. Tabar, I.K. Mellinghoff, L.M. DeAngelis, C.E. Ariyan, N. Lee, W.D. Tap, M.M. Gounder, S.P. D'Angelo, L. Saltz, Z.K. Stadler, H.I. Scher, J. Baselga, P. Razavi, C.A. Klebanoff, R. Yaeger, N.H. Segal, G.Y. Ku, R.P. DeMatteo, M. Ladanyi, N.A. Rizvi, M.F. Berger, N. Riaz, D.B. Solit, T.A. Chan, L.G.T. Morris, Tumor mutational load predicts survival after immunotherapy across multiple cancer types, Nat. Genet. 51 (2019) 202–206, https://doi.org/10.1038/s41588-018-0312-8.
[20] A.M. Goodman, S. Kato, L. Bazhenova, S.P. Patel, G.M. Frampton, V. Miller, P.J. Stephens, G.A. Daniels, R. Kurzrock, Tumor mutational burden as an independent predictor of response to immunotherapy in Diverse cancers, Mol. Cancer Therapeut. 16 (2017) 2598–2608, https://doi.org/10.1158/1535-7163.Mct-17-0386.
[21] Q. Xu, H. Xu, R. Deng, Z. Wang, N. Li, Z. Qi, J. Zhao, W. Huang, Multi-omics analysis reveals prognostic value of tumor mutation burden in hepatocellular carcinoma, Cancer Cell Int. 21 (2021) 342, https://doi.org/10.1186/s12935-021-02049-w.
[22] D.J. McGrail, P.G. Pilié, N.U. Rashid, L. Voorwerk, M. Slagter, M. Kok, E. Jonasch, M. Khasraw, A.B. Heimberger, B. Lim, N.T. Ueno, J.K. Litton, R. Ferrarotto, J. T. Chang, S.L. Moulder, S.Y. Lin, High tumor mutation burden fails to predict immune checkpoint blockade response across all cancer types, Ann. Oncol. 32 (2021) 661–672, https://doi.org/10.1016/j.annonc.2021.02.006.
[23] V.S. LeBleu, Imaging the tumor microenvironment, Cancer J. 21 (2015) 174–178, https://doi.org/10.1097/PPO.0000000000000118.
[24] C. Pottier, A. Wheatherspoon, P. Roncarati, R. Longuespée, M. Herfs, A. Duray, P. Delvenne, P. Quatresooz, The importance of the tumor microenvironment in the therapeutic management of cancer, Expert Rev. Anticancer Ther. 15 (2015) 943–954, https://doi.org/10.1586/14737140.2015.1059279.
[25] D.C. Hinshaw, L.A. Shevde, The tumor microenvironment Innately Modulates cancer progression, Cancer Res. 79 (2019) 4557–4566, https://doi.org/10.1158/0008-5472.CAN-18-3962.
[26] Z. Liu, Y. Lin, J. Zhang, Y. Zhang, Y. Li, Z. Liu, Q. Li, M. Luo, R. Liang, J. Ye, Molecular targeted and immune checkpoint therapy for advanced hepatocellular carcinoma, J. Exp. Clin. Cancer Res. 38 (2019) 447, https://doi.org/10.1186/s13046-019-1412-8.
[27] J.M. Llovet, R. Montal, D. Sia, R.S. Finn, Molecular therapies and precision medicine for hepatocellular carcinoma, Nat. Rev. Clin. Oncol. 15 (2018) 599–616, https://doi.org/10.1038/s41571-018-0073-4.
[28] T.D. Fischer, J.H. Wang, A. Vlada, J.S. Kim, K.E. Behrns, Role of autophagy in differential sensitivity of hepatocarcinoma cells to sorafenib, World J. Hepatol. 6 (2014) 752–758, https://doi.org/10.4254/wjh.v6.i10.752.
[29] F.Q. Wu, T. Fang, L.X. Yu, G.S. Lv, H.W. Lv, D. Liang, T. Li, C.Z. Wang, Y.X. Tan, J. Ding, Y. Chen, L. Tang, L.N. Guo, S.H. Tang, W. Yang, H.Y. Wang, ADRB2 signaling promotes HCC progression and sorafenib resistance by inhibiting autophagic degradation of HIF1α, J. Hepatol. 65 (2016) 314–324, https://doi.org/10.1016/j.jhep.2016.04.019.
[30] X. Sun, X. Niu, R. Chen, W. He, D. Chen, R. Kang, D. Tang, Metallothionein-1G facilitates sorafenib resistance through inhibition of ferroptosis, Hepatology 64 (2016) 488–500, https://doi.org/10.1002/hep.28574.
[31] W. Tang, Z. Chen, W. Zhang, Y. Cheng, B. Zhang, F. Wu, Q. Wang, S. Wang, D. Rong, F.P. Reiter, E.N. De Toni, X. Wang, The mechanisms of sorafenib resistance in hepatocellular carcinoma: theoretical basis and therapeutic aspects, Signal Transduct. Targeted Ther. 5 (2020) 87, https://doi.org/10.1038/s41392-020-0187-x.
[32] J.Y. Wu, J.Z. Yao, S. Jia, X.K. Yao, J.P. Shao, X.M. Yao, H. li, PREPRINT (Version 1), A cuproptosis-related lncRNA signature for predicting prognosis and immune response in hepatocellular carcinoma (2022), https://doi.org/10.21203/rs.3.rs-2142200/v1. Research Square.